RC 20831 (05/2/97)

Physical Sciences

IBM Research Report

Metallization Induced Band Bending of $SrTiO_3(100)$ and $Ba_{0.7}Sr_{0.3}TiO_3$

M. Copel, P. R. Duncombe, D. A. Neumayer, T. M. Shaw, R. M. Tromp

IBM Research Division

T.J. Watson Research Center

Yorktown Heights, New York

Research Division

Almaden · T.J. Watson · Tokyo · Zurich

Metallization Induced Band Bending of $SrTiO_3(100)$ and $Ba_{0.7}Sr_{0.3}TiO_3$

M. Copel, P. R. Duncombe, D. A. Neumayer, T. M. Shaw, R. M. Tromp

IBM Research Division, T. J. Watson Research Center

P.O. Box 218, Yorktown Heights, NY 10598

(October 8, 1997)

Abstract

We have investigated the interaction of Pt with single-crystal $SrTiO_3(001)$ and polycrystalline $Ba_{0.7}Sr_{0.3}TiO_3$ thin films using photoemission spectroscopies. Significant band bending is caused by interface formation, determining the Schottky barrier height. We have depth profiled the band-bending for $Ba_{0.7}Sr_{0.3}TiO_3$ thin films, giving a direct measurement of the depletion depth and built-in potential.

Ms number xxx PACS numbers: 73.30.+y, 73.40.Ns, 77.55.+f, 77.84.Bw

The need for high dielectric-constant materials for charge storage has driven research in titanate thin films. In the bulk paraelectric phase, $Ba_{0.7}Sr_{0.3}TiO_3$ (BST) exhibits a dielectric constant as high as 2.6×10^3, but thin film capacitors generally show permitivities an order of magnitude lower. The insulator/metal junction is quite important for device characteristics; for example, an undesireable interfacial capacitance of unknown origin is commonly observed, which ultimately dominates the permitivity in the thin film limit [1–4]. In addition, it is believed that leakage characteristics are strongly influenced by the Schottky barriers at the insulator/metal junctions. The barrier height determines the rate of thermionic emission of charge carriers into the dielectric [5]. Thus, there are two motivations for studying band bending at ferroelectric/metal junctions. First, there is the need to quantify the barrier height and optimize leakage characteristics. A second goal is to examine the effect of metallization on dielectric properties, since the internal fields induced by Schottky barrier formation may reduce the permitivity, thus causing the mysterious interfacial capacitance [6]. To date, there have been no measurements of metal induced band-bending of $SrTiO_3$ or BST, although Schottky barrier heights for a number of metals on $SrTiO_3$ have been determined by electrical characterization [5].

The band-bending that accompanies metal deposition on $SrTiO_3$ and BST can be determined by core level shifts observed with x-ray photoelectron spectroscopy (XPS). The photoemission process imposes a rigid translation of core-level binding energies to photoelectron kinetic energies. When barrier formation shifts the bands towards smaller binding energy, the core levels are likewise shifted and the photoelectrons have a higher kinetic energy. Since the depletion depth greatly exceeds the photoelectron mean free path, as we will show below, we can neglect the variation in band-bending within the region sampled by photoemission.

Several types of samples were used in this study. For $SrTiO_3$, n-type (100) crystals (0.5 and 0.05 wt. % Nb) were purchased from Nikko Hitech. Before mounting, samples were etched for 15 min. in 40% NH_4F solution to eliminate any residual polishing grit. Samples were slowly heated in ultra-high vacuum to 680°C, then oxidized at 680°C in 10^{-3} torr O_2

for 10 min. in a turbo-pumped side-chamber. This resulted in clean surfaces with a (1×1) low energy electron diffraction pattern and no observable surface carbon. Samples were allowed to cool overnight before data acquisition. Pt was deposited *in situ* from an e-beam evaporator that operated at a pressure of 10^{-9} torr at a rate of 0.2 monolayers/min. Pt coverages were calibrated using medium energy ion scattering. After depositions, samples were allowed to thermally equilibrate for at least 1 hour.

Polycrystalline BST films were fabricated either by chemical solution deposition (CSD) [7,8] or metal-organic chemical vapor deposition (MOCVD) in a Varian high dielectric constant reactor [9]. The CSD synthesis was from barium, strontium and titanium 2-methoxyethoxides dissolved in 2-methoxyethanol, which was spun onto Pt coated, oxidized Si wafers with a Ti adhesion layer. The layers underwent a 700°C rapid thermal anneal in an oxygen ambient. Similar substrates were used for MOCVD, but the Ti layer was omitted. Both types of BST films were *in situ* annealed and oxidized as described above, but at 600°C.

Photoemission spectra were taken using a Leybold-Hereaus EA11 hemispherical analyzer. XPS measurements used Mg Kα radiation with the sample aligned to a 45° exit angle. Valence band ultra-violet photoemission spectra (UPS) were obtained by He I radiation, with the sample aligned to normal emission. Kinetic energies were calibrated using the Ti 2p1/2 core level from a sputter-cleaned polycrystalline Ti foil. Two experimental difficulties were encountered on undoped films: First, prolonged exposure to an x-ray flux induced core-level shifts on some samples, probably due to impurity traps. We were able to avoid this effect by minimizing exposure times. Second, charging effects were observed on the most highly insulating samples, which were corrected by using the Pt 4f core level as a reference standard.

Valence band UPS spectra prior to metallization show a broad gap (Fig. 1). (The small density of states above the valence band maximum is an artifact of the He resonance lamp.) Following ref. [10,11], we place the valence band maximum about 3 eV below the Fermi level. Since $SrTiO_3$ as well as BST has a gap of 3.1 eV at room temperature, the Fermi level is within a few hundred millivolts of the conduction band minimum. This result agrees with the known carrier density of the sample (5×10^{18} cm^{-3}). Upon deposition of 2 monolayers of Pt, the UPS spectrum becomes metallic, with a sharp cutoff at the Fermi level. In the same figure we have included a spectrum from a nominally undoped polycrystalline BST thin film. Despite the absence of deliberately introduced dopants, the bare surface of the film is n-type.

Information about band-bending can be derived from XPS core-level shifts (Fig. 2). Upon deposition of Pt, a steep increase in core level kinetic energy is observed, forming a plateau after the first monolayer. Since the Ti 2p3/2 level, the Sr 3d doublet and the O 1s level all undergo the same shift, we can be assured that the shift is caused by band-bending rather than chemical effects. Combining XPS and UPS observations, we deduce that after metallization the conduction band minimum resides 0.55 and 0.65 eV above the Fermi level for $SrTiO_3$(100) 0.5 and 0.05 wt. % Nb, forming a Schottky barrier. Qualitatively similar results are found for undoped 880Å $SrTiO_3$ thin films fabricated by CSD techniques. But for undoped $SrTiO_3$, we see a Schottky barrier of roughly 0.8 eV. This is lower than the 1.2 eV barrier found in electrical measurements [5]. The Schottky barrier for thin film samples does not change significantly if we introduce 0.1 at. % Ni, an acceptor dopant. Finally, we note that very little band bending is observed for Au metallization of n-type $SrTiO_3$.

Our results can be understood in the context of what has been learned for semiconductor Schottky barrier formation [12]. There is a large difference between the work function of Pt (5.7 eV) and the electron affinity level of $SrTiO_3$, so significant band-bending is required to equilibrate the Fermi-levels. We expect to find less band-bending if we raise the metal Fermi level. Au has a work function of 5.3 eV, so the metal Fermi level is quite close to the electron affinity level of $SrTiO_3$ and little band-bending is required to reach equilibrium.

Now we extend our results to the more technologically relevant case of BST. Measurements on nominally undoped BST thin films show band bending that is similar to results for undoped $SrTiO_3$. The core levels shift towards higher kinetic energy upon metallization (Fig. 3a), and the final Ti 2p3/2 core is nearly the same as observed on undoped $SrTiO_3$.

Interestingly, the initial position of the Ti 2p3/2 core level depends on the film thickness. This is due to the influence of the underlying Pt layer, which also bends the bands. We can "depth-profile" the band bending by plotting the Ti 2p3/2 position prior to metallization as a function of film thickness (Fig. 3b). To model the results, we must keep in mind that the field strength increases linearly across the film, with the maximum at the metal/insulator interface and no electric field at the vacuum/insulator interface (Fig. 3c). Thus, a film that is thinner than the depletion width, W, will have an internal electric field of $2(t-x)V_{bi}/W^2$, where x is the distance from the metal/insulator interface, and V_{bi} is the built-in potential. Integrating to a film thickness of t, we obtain

$$V_{ob} = V_{int} - t^2 \times V_{bi}/W^2 \tag{1}$$

where V_{ob} is the observed Ti 2p3/2 kinetic energy, V_{int} is the interface value of Ti 2p3/2 kinetic energy, and t is less than W, the depletion width. The optimized values of W and V_{bi} are 700 Å and 0.5 eV and 1300 Å and 0.3 eV for MOCVD and CSD films, respectively. We note that the depletion depths are two orders of magnitude greater than the escape depths for photoelectrons.

Let us return to the results for undoped $SrTiO_3$. Prior to metallization, the Ti 2p3/2 has a higher kinetic energy on undoped $SrTiO_3$ than n-type $SrTiO_3$(100). Unfortunately, we cannot determine whether this is caused by back-contact pinning or a change in the bulk Fermi-level, unless a series of film thicknesses are examined. In both cases, the core levels are shifted towards higher kinetic energies. To deduce the bulk Fermi level position, we must insure that the film is thicker than the depletion depth.

Finally, we consider the effect of the built-in potential on the dielectric properties of BST films. For films thicker than $2 \times W$, the built-in electric field of the depletion region should reduce the permitivity near the interface, observed as an interfacial capacitance. But if the film is thinner than $2 \times W$, the depletion regions of the front and back contacts overlap, and simple electrostatic considerations dictate that the built-in electric field *decreases* as the film becomes thinner. Consequently, the effect of the built-in field on the film's dielectric constant should vanish in the thin film limit. But an interfacial capacitance is observed for films much thinner than $2 \times W$, and it does not vary with film thickness. Thus, we infer that the mysterious interfacial capacitance is not caused by interfacial band-bending.

In conclusion, we have demonstrated that Pt metallization on $SrTiO_3$ and BST results in substantial band-bending that determines the Schottky barrier height. There is a greater barrier height on undoped and lightly acceptor doped $SrTiO_3$ than on heavily donor doped $SrTiO_3(100)$. This is surprising, since the conventional model of Schottky barrier formation predicts a barrier independent of doping. BST and $SrTiO_3$ thin films show nearly identical barriers. Consideration of the size of the depletion region has lead us to discard the effects of the built-in potential on thin-film dielectric properties.

The authors thank R. Haight and J. Tersoff for helpful discussions. We also acknowledge D. Kotecki, R. Waser and S. Hoffman for samples. MOCVD samples were provided under the Ultra-Dense Capacitor Materials Processing Partnership sponsored by DARPA under contract No. MDA-972-93-C-0033.

REFERENCES

[1] S. Yamamishi, T. Sakuma, K. Takemura and Y. Miyasaka, J. Jour. Appl. Phys. **30**, 2193 (1991).

[2] K. Abe and S. Komatsu, J. Jour. Appl. Phys. Part I**31**, 2985 (1992); K. Abe and S. Komatsu, J. Jour. Appl. Phys. Part I **32**, 1157L (1993).

[3] For a discussion, see R. Waser, Integrated Ferroelectrics, *in press* and references therein.

[4] C. Basceri, S. K. Streiffer, A. Kingon and R. Waser, J. Appl. Phys. *in press.*

[5] G. W. Dietz, W. Antpohler, M. Klee and R. Waser, J. Appl. Phys. **78**, 6113 (1995).

[6] K. M. Jordan, J. Appl. Phys. **33**, 2826 (1962).

[7] D. A. Neumayer, P. R. Duncombe, R. Laibowitz, and A. Grill, ISIF conference proceedings, March, 1997, Santa Fe, New Mexico.

[8] J. F. Campion, D. A. Payne, H. K. Chae, and Z. Xu, Ceramic Transactions, **22**, 477 (1991).

[9] P. C. Van Buskirk, J. F. Roeder and S. Bilodeau, Integrated Ferroelectrics, **10**, 9 (1995).

[10] V. E. Henrich, G. Dresselhaus, and H. J. Zeiger, Phys. Rev. B **17**, 4908 (1978).

[11] B. Reihl, J. G. Bednorz, K. A. Muller, Y. Jugnet, G. Landgren, and J. F. Morar, Phys. Rev. B **30**, 803 (1984).

[12] S. M. Sze, *Semiconductor Devices, Physics and Technology* (John Wiley & Sons, New York, 1985) p. 245.

FIGURES

FIG. 1. Ultra-violet photoemission spectra for n-type $SrTiO_3$ and undoped BST before and after deposition of 2 monolayers of Pt.

FIG. 2. Core level kinetic energies of $SrTiO_3$ as a function of Pt coverage. The shifts are caused by band-bending that accompanies metallization.

FIG. 3. a) Ti 2p3/2 core level kinetic energy for nominally undoped BST thin films as a function of Pt coverage. The films are supported by a Pt coated substrate. b) Ti 2p3/2 initial position as a function of film thickness. Since the Pt substrate forms a back contact, the plot reveals a depth profile of the band-bending. c) Model of the film thickness dependence of the electric field and band offset.

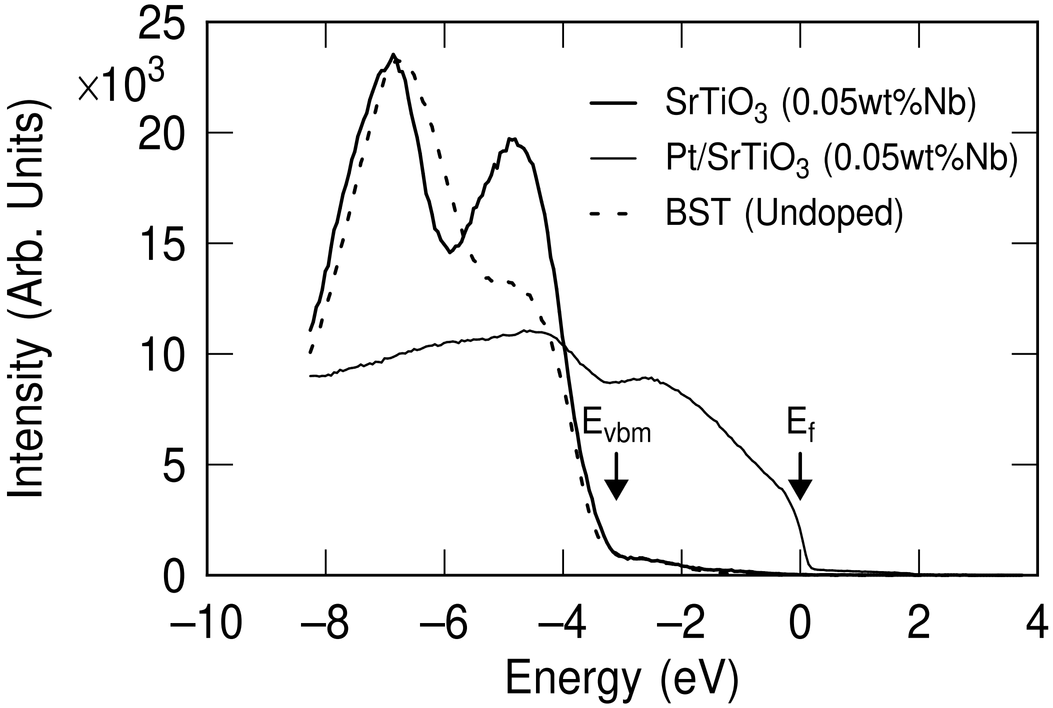

25
×10^3
20
15
10
5
0
−10
−8
−6
−4
−2
0
2
4
Energy (eV)
Intensity (Arb. Units)
SrTiO3 (0.05wt%Nb)
Pt/SrTiO3 (0.05wt%Nb)
BST (Undoped)
Evbm
Ef

FIGURE 1

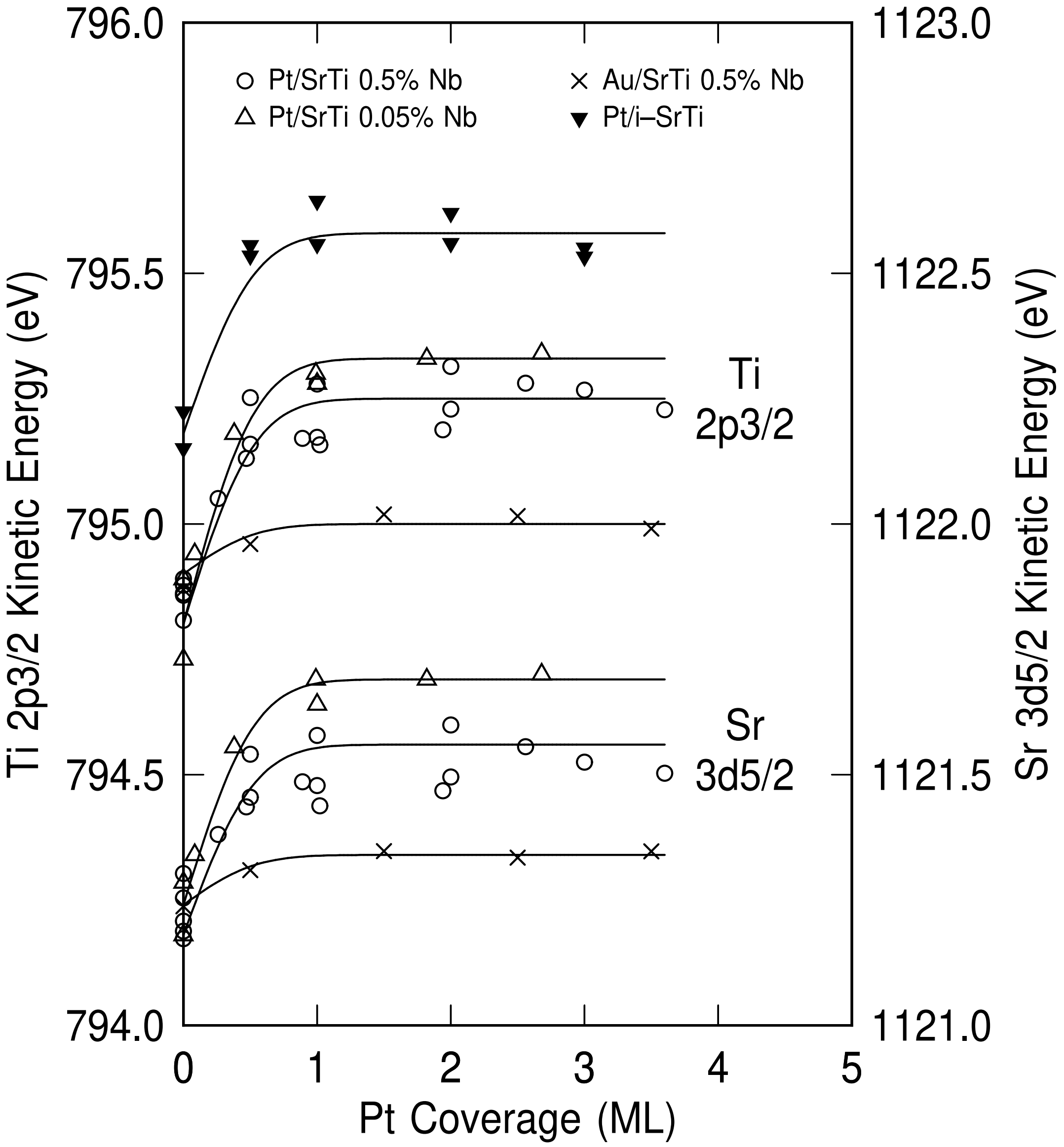
796.0
795.5
795.0
794.5
794.0
1123.0
1122.5
1122.0
1121.5
1121.0
0
1
2
3
4
5
Pt/SrTi 0.5% Nb
Pt/SrTi 0.05% Nb
Au/SrTi 0.5% Nb
Pt/i–SrTi
Ti
2p3/2
Sr
3d5/2
Ti 2p3/2 Kinetic Energy (eV)
Sr 3d5/2 Kinetic Energy (eV)
Pt Coverage (ML)

FIGURE 2

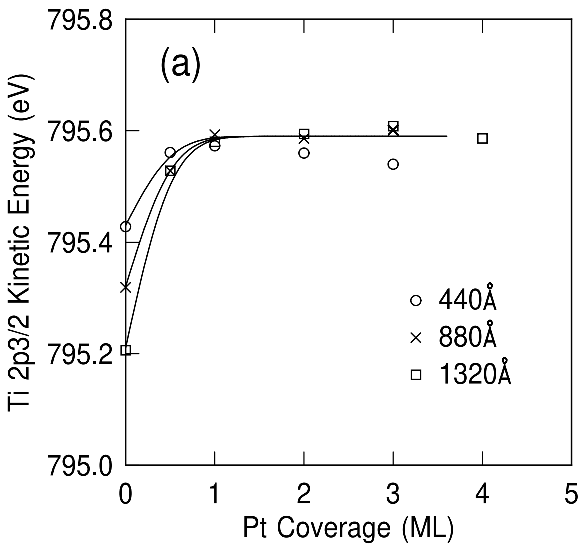
(a)
Ti 2p3/2 Kinetic Energy (eV)
795.8
795.6
795.4
795.2
795.0
0
1
2
3
4
5
Pt Coverage (ML)
440Å
880Å
1320Å

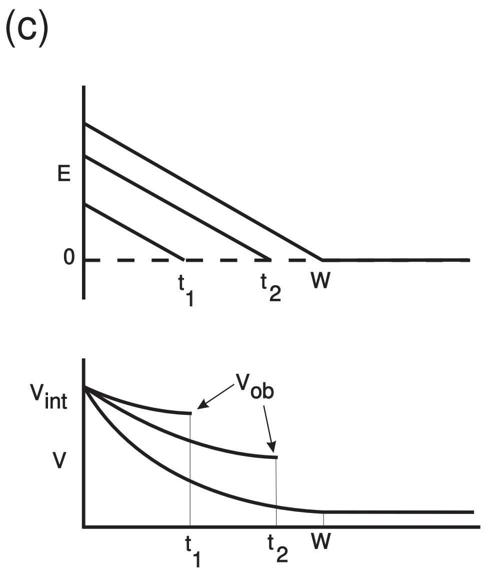
(c)
E
0
t1
t2
W
Vint
Vob
V
t1
t2
W

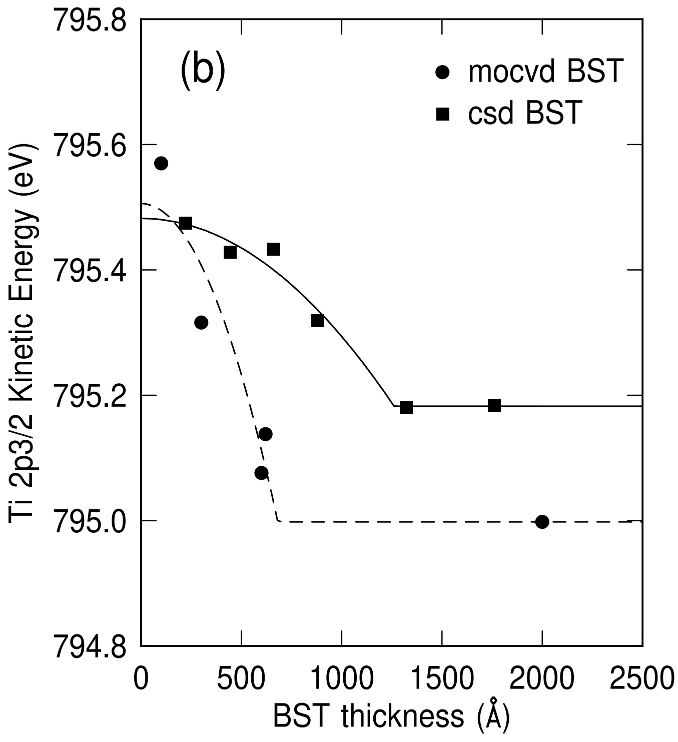
(b)
mocvd BST
csd BST
Ti 2p3/2 Kinetic Energy (eV)
795.8
795.6
795.4
795.2
795.0
794.8
0
500
1000
1500
2000
2500
BST thickness (Å)

FIGURE 3